Cardiovascular Control: Cardiovascular haemodynamics and ventriculo-arterial coupling in an acute pig model of coronary ischaemia–reperfusion

Lieve Lanoye, Patrick Segers, Vincent Tchana-Sato, Stephanie Rolin, Jean-Michel Dogne, Alexandre Ghuysen, Bernard Lambermont, Julien Hanson, Thomas Desaive, Pascal Verdonck, Vincent D'Orio and Philippe Kolh

Exp Physiol 2007;92;127-137; originally published online Oct 12, 2006;

DOI: 10.1113/expphysiol.2006.034983

Experimental Physiology

Cardiovascular haemodynamics and ventriculo-arterial coupling in an acute pig model of coronary ischaemia–reperfusion

Lieve Lanoye[1], Patrick Segers[1], Vincent Tchana-Sato[2], Stephanie Rolin[3], Jean-Michel Dogne[3], Alexandre Ghuysen[2], Bernard Lambermont[2], Julien Hanson[4], Thomas Desaive[5], Pascal Verdonck[1], Vincent D'Orio[2] and Philippe Kolh[2]

[1]*Cardiovascular Mechanics and Biofluid Dynamics, Institute Biomedical Technology, Ghent University, Belgium*
[2]*Haemodynamic Research Center (HemoLiège),* [3]*Department of Pharmacy, University of Namur, Belgium,* [4]*Department of Medicinal Chemistry and* [5]*Thermodynamics of Irreversible Processes, University of Liège, Belgium*

Although reperfusion after coronary occlusion is mandatory for myocardial salvage, reperfusion may trigger a cascade of harmful events (reperfusion injury) adding to myocardial injury. We investigated effects of reperfusion on left ventricular (LV) haemodynamics and ventriculo-arterial (VA) coupling in pigs following acute myocardial ischaemia induced by coronary artery occlusion. Experiments were performed in six animals, with measurements of cardiac and arterial function at baseline, after 60 min of ischaemia (T60) and after 2 (T180) and 4 h of reperfusion (T300). Ventriculo-arterial coupling was assessed using the ventriculo-arterial elastance ratio of paper, as well as using a 'stiffness coupling' and 'temporal coupling' index. Reperfusion following ischaemia (T180 *versus* T60) induced a progressive decline in cardiovascular function, evidenced by a decrease in mean arterial blood pressure, cardiac output and ejection fraction which was not restored at T300. Although reperfusion also induced an increase in slope of the end-systolic pressure–volume relationship (ESPVR), the ESPVR curve shifted to the right, associated with a depression of contractile function. Histology demonstrated irreversible myocardial damage at T300. The ventriculo-arterial elastance ratio and the 'stiffness coupling' index were unaffected throughout the protocol, but the 'temporal coupling' parameter indicated a relative shift between heart period and the time constant of the arterial system. It is unlikely that these alterations are attributable to ischaemic injury alone. The combination of both the stiffness and temporal coupling index may provide more information when studying ventriculo-arterial coupling than the more commonly used ventricular end-systolic stiffness/effection arterial elastance (E_{es}/E_a) ratio.

(Received 10 July 2006; accepted after revision 9 October 2006; first published online 12 October 2006)
Corresponding author L. Lanoye: Hydraulics Laboratory, Institute Biomedical Technology, St-Pietersnieuwstraat 41, 9000 Gent, Belgium. Email: lieve.lanoye@ugent.be

Myocardial ischaemia in the clinical setting is often a consequence of a thrombotic occlusion of a coronary artery at the site of a ruptured atherosclerotic plaque or downstream from it. It appears obvious that prompt re-establishment of coronary flow following coronary occlusion is mandatory for the preservation of myocardial tissue and to decrease postmyocardial infarction mortality (Boersma *et al.* 1996; Newby, 1997). It has, however, been demonstrated that even after early initiation of successful reperfusion, myocardial damage may still occur (Hearse *et al.* 1975; Opie, 1989). This prevalence of damage even after reperfusion, along with other observations, revealed that, although reperfusion is needed for myocardial salvage, it may also trigger a cascade of harmful events which add to myocardial injury. The part of the myocardial injury and the clinical manifestations specifically triggered by reperfusion have been labelled as 'reperfusion injury' (Hearse *et al.* 1975; Opie, 1989).The issue of reperfusion injury is still not fully understood. On the one hand, it has been suggested that the impact of reperfusion only accelerates the expression of irreversible myocardial damage caused by ischaemia,

DOI: 10.1113/expphysiol.2006.034983

but does not cause any damage in itself. On the other hand, however, there is evidence that the ischaemic myocardium remains still viable at the end of reasonably long ischaemic periods (Cerra *et al.* 1975). The latter evidence suggests that irreversible injury caused by the reperfusion itself (and not the prolonged ischaemia) is indeed a true phenomenon. This concept, where reperfusion induces further injury, also has support from infarct-limiting effects of pharmacological interventions initiated immediately before or at the onset of reperfusion (Higo *et al.* 1993; Wang *et al.* 2002); if the damage were solely the result of ischaemia, these pharmacological agents would have no effect at all.

Reperfusion injuries have mostly been assessed at the cellular level, and the direct causes of necrosis and apoptosis have been studied at the molecular level. Many different mechanisms of reperfusion-induced cell damage and cell death have been identified. For example, oxidants and free radicals play an important role in reperfusion injury (Zweier & Talukder, 2006). In addition, cell damage caused by Ca^{2+} overload-induced contracture and reoxygenation-induced rigor contracture is observed (Piper *et al.* 2004).

Nonetheless, it is equally important to study the overall cardiovascular changes that result from the ischaemia–reperfusion-induced mechanisms. Some more recent studies have focused on the influence of ischaemia and reperfusion on circulatory parameters in pigs (Kamimura *et al.* 2003; Khalil *et al.* 2005; Metzsch *et al.* 2006). In all these studies, however, only a limited haemodynamic analysis was performed, and the studies did not incorporate pressure–volume analysis or ventriculo-arterial coupling, which enable assessment of the 'matching' between cardiac and arterial parameters that results in a working point of the cardiovascular system (producing a certain cardiac output and blood pressure) and its associated energetic cost.

The primary aim of this study was to gain insight into and document the wide range of alterations in haemodynamics induced by prolonged ischaemia and subsequent reperfusion. We chose to perform the experiment in a large animal model with coronary structure and function closely resembling those of humans. Focusing on ventriculo-arterial function and coupling, we analysed our data in terms of the 'classical' ventriculo-arterial elastance, as well as in terms of a recently proposed coupling concept using both a stiffness and a temporal coupling index.

Methods

Animal preparation

All experimental procedures and protocols used in this investigation were reviewed and approved by the Ethics Committee of the Medical Faculty of the University of Liège. All procedures conformed to the Guiding Principles in the Care and Use of Animals of the American Physiological Society and were performed according to the *Guide for the Care and Use of Laboratory Animals* (NIH publication no. 85–23, revised 1996).

Experiments were performed on six healthy pure pietran pigs of either sex (20–28 kg). The animals were premedicated with intramuscular administration of ketamine ($20\ mg\ kg^{-1}$) and diazepam ($1\ mg\ kg^{-1}$). Anaesthesia was then induced and maintained by a continuous infusion of sufentanil ($0.5\ \mu g\ kg^{-1}\ h^{-1}$) and sodium pentobarbitone ($3\ mg\ kg^{-1}\ h^{-1}$). Spontaneous movements were prevented by pancuronium bromide ($0.1\ mg\ kg^{-1}$). After endotracheal intubation through a cervical tracheostomy, the pigs were connected to a volume-cycled ventilator (Evita 2, Dräger, Lübeck, Germany) set to deliver a tidal volume of $10\ ml\ kg^{-1}$ at a respiratory rate of $20\ min^{-1}$. Measurements of end-tidal partial pressure of CO_2 (Capnomac, Datex, Helsinki, Finland) were used to monitor the adequacy of ventilation. Respiratory settings were adjusted to maintain end-tidal CO_2 in the range of 35–40 mmHg (4.67–5.33 kPa). Arterial oxygen saturation was closely monitored and maintained above 95% by adjusting the fractional inspired O_2 as necessary. Core temperature was measured with a rectal probe and maintained at 37°C by means of a heating blanket. A standard lead electrocardiogram was used for the monitoring of heart rate (HR).

The chest was entered through median sternotomy, the pericardium was incised and sutured to the chest wall to form a cradle for the heart, and the root of the aorta was dissected clear of adherent fat and connective tissue. A combined conductance–micromanometer catheter (CD Leycom, Zoetermeer, The Netherlands) was inserted through the right carotid artery and advanced into the left ventricle. A micromanometer-tipped catheter (Sentron pressure measuring catheter, Cordis, Miami, FL, USA) was inserted through the right femoral artery and advanced into the ascending aorta. A 14 mm diameter perivascular flow probe (Transonic Systems Inc., Ithaca, NY, USA) was closely adjusted around the aorta 2 cm downstream to the aortic valve. The micromanometer-tipped catheter was manipulated so that the pressure sensor was positioned just distal to the flow probe. Right atrial pressure was measured with a micromanometer-tipped catheter inserted into the cavity through the superior vena cava. A 2.0 mm Fogarty balloon catheter (Baxter Healthcare Corp., Oakland, CA, USA) was advanced into the inferior vena cava through a right femoral venotomy. Inflation of this balloon produced a leftward shift in pressure–volume (P–V) loops by reducing venous return. Thrombus formation along the catheters was prevented by administration of 100 i.u. kg^{-1} of heparin sodium intravenously just before the catheter insertion.

A segment of the left anterior descending (LAD) coronary artery was isolated distal to the first diagonal branch for later application of a surgical clamp. An electromagnetic flow probe (Transonic Systems Inc.) was placed around the LAD coronary artery 3 cm distal to the site of occlusion, to verify the occlusion (complete loss of coronary artery blood flow). In case of occurrence of ventricular fibrillation, animals were defibrillated at 1 J kg^{-1} using internal paddles.

Experimental protocol

The animals were continuously infused intravenously with Ringer lactate solution (5 ml kg^{-1} h^{-1}), and, when necessary, with hydroxyethyl starch (6%) to maintain central venous pressure up to 6–7 mmHg over 30 min. After placement of all instrumentation and verification of their proper functioning, animals were allowed to equilibrate for an additional 30 min, after which baseline (BL) recordings were made. Thereafter, the LAD coronary artery was occluded at the site of previous dissection for 1 h, and measurements were repeated before coronary perfusion was restored (T60). Subsequent measurements were repeated after 2 (T180) and 4 h of reperfusion (T300; Fig. 1*A*).

Haemodynamic data collection

The conductance catheter was connected to a Sigma-5 signal-conditioner processor (CD Leycom). Each ultrasonic flow probe was connected to a flowmeter (HT 207, Transonic Systems Inc.), and each micromanometer-tipped catheter to the appropriate monitor (Sentron pressure monitoring). All analog signals and the ventricular pressure–volume loops were displayed on screen for continuous monitoring. The analog signals were continuously converted to digital form with appropriate software (Codas, DataQ Instruments Inc., Akron, OH, USA) at a sampling frequency of 200 Hz.

Ventricular systolic function and energetics. Ventricular systolic function was assessed through different parameters. Left ventricular volumes were inferred using the dual field conductance catheter technique (Baan *et al.* 1984; Steendijk *et al.* 1993). Calibration of the conductance signal to obtain absolute volume was performed by the hypertonic saline method (Baan *et al.* 1984). Therefore, a small volume (1–2 ml) of 10% NaCl solution was injected into the pulmonary artery during continuous data acquisition. Stroke volume (SV) was calculated from steady-state recordings as the difference between end-diastolic (EDV) and end-systolic volume (ESV). Cardiac output (CO) was calculated as the product of heart rate (HR) and SV. Ejection fraction (EF) was calculated as SV/EDV. Left ventricular contractile function was assessed by the end-systolic pressure–volume relation (ESPVR) (Suga *et al.* 1979), and the preload recruitable stroke work (PRSW) relation (Glower *et al.* 1985). Both indices require pressure–volume loops

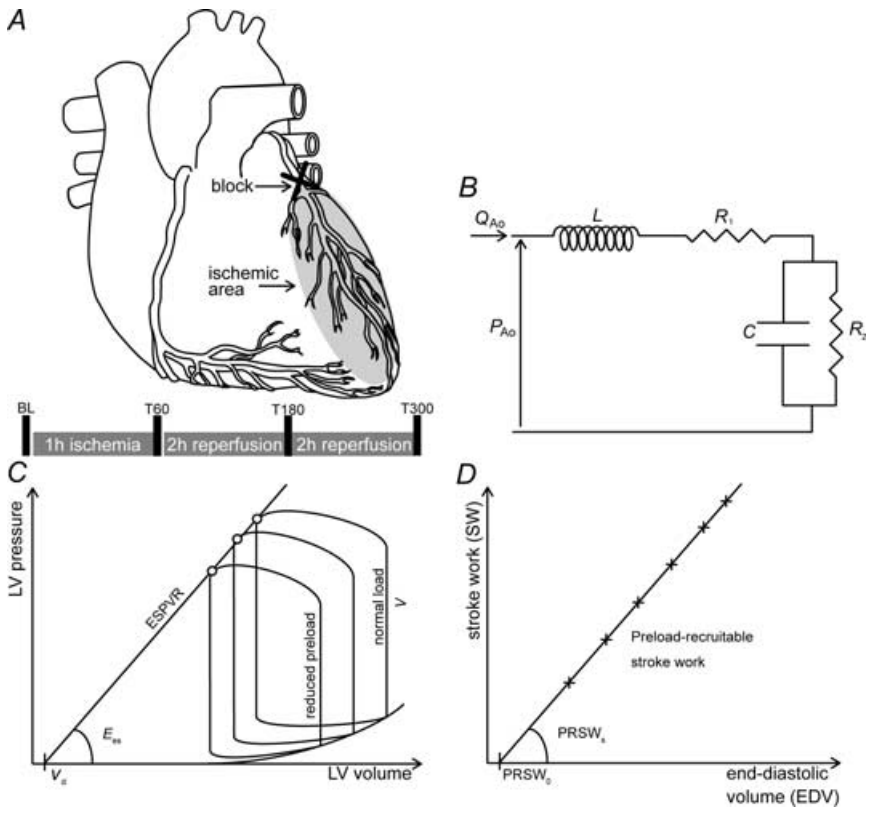

Figure 1. Protocol and assessment of arterial and ventricular function parameters
A, protocol used in this study. *B*, the four-element windkessel model used to assess the vascular properties. *C*, how end-systolic elastance (E_{es}) and dead volume (V_d) were assessed from caval occlusion. *D*, how the preload-recruitable stroke work curve was assessed from the PV loops in *C*. Q_{Ao}, aortic flow; P_{Ao}, aortic pressure.

(PV loops) measured under gradual preload decline obtained through inhibition of venous return (Fig. 1*D*). All measurements were taken immediately after the animal was disconnected from the ventilator to sustain end expiration. The caval occlusion was limited to a few seconds to avoid reflex responses. The instantaneous pressure–volume relationship was considered in terms of a time-varying elastance $E(t)$, defined by:

$$E(t) = \frac{P(t)}{V(t) - V_{\mathrm{d}}}$$

where $P(t)$ and $V(t)$ are, respectively, the instantaneous ventricular pressure and volume; dead volume, V_{d}, is a correction term. End systole was defined as the instant of time in the ejection phase at which $E(t)$ reaches its maximum, $E_{\max}$. It has been demonstrated that $E(t)$ and V_{d} are insensitive to preload, at least within physiological ranges (Suga *et al.* 1979). Stroke work (SW) was calculated as the area enclosed within each pressure–volume loop and was plotted against EDV to generate the SW–EDV relation (preload recruitable stroke work, PRSW).

Myocardial energetics were assessed by computation of pressure–volume area (PVA) using steady-state measurements. In the time-varying elastance model of the ventricle, the total energy generated by each contraction is represented by the total area under the end-systolic pressure–volume relation line and the systolic segment of the pressure–volume loop, and above the end-diastolic pressure–volume relation curve, and denoted by PVA (Suga *et al.* 1979). Pressure–volume area is the sum of SW, or the energy that the ventricle delivers to the blood at ejection, and potential energy (PE), necessary to overcome the viscoelastic properties of the myocardium itself. It has been demonstrated that PVA is highly correlated with myocardial oxygen consumption (Denslow, 1996). Mechanical efficiency is defined as the SW/PVA ratio.

Arterial function. Arterial properties were assessed from ascending aortic pressure and flow measurements during steady-state conditions and represented with a four-element windkessel model (WK4; see Fig. 1*B*; Lambermont *et al.* 1998). In this WK4 model, the resistor R_2 represents the resistive properties of the systemic bed, which reside primarily in the arteriolar system. The capacitor, C, placed in parallel with R_2, represents the compliant properties of the systemic vessels. The resistor R_1 represents the characteristic impedance, the level of which depends predominently on the elastic properties of the proximal aorta. Finally, an inductance, L, is introduced to take blood inertia into account. Furthermore, L restores positive phase angles at high frequencies of the impedance spectrum (Grant & Paradowski, 1987). The values of R_1, R_2, C and L were estimated by a previously described method (Lambermont *et al.* 1998). Effective arterial elastance (E_{a}) was calculated according to the equation (Sagawa *et al.* 1988):

$$E_{\mathrm{a}} = \frac{R_1 + R_2}{T_{\mathrm{s}} + R_2 C\,(1 - e^{-T_{\mathrm{d}}/R_2 C})}$$

where T_{s} and T_{d} are the systolic and diastolic time intervals, respectively. In the aortic pressure wave, T_{s} was calculated as the time interval between the point just before the abrupt rise and the dicrotic notch.

Ventriculo-arterial coupling. Ventriculo-arterial (VA) coupling was first studied through the ratio $E_{\mathrm{es}}/E_{\mathrm{a}}$, where E_{es} is the ventricular end-systolic stiffness. It has, however, been demonstrated by Stergiopulos *et al.* (1996) and Segers *et al.* (2002) that VA coupling can be described in more detail using two dimensionless parameters, i.e. a 'stiffness coupling index', calculated as the ratio of E_{es} and arterial stiffness ($1/C$), yielding $E_{\mathrm{es}}C$, and the 'temporal coupling index', calculated as the ratio of the time constant of the arterial system (R_2C) and the heart period (T), R_2C/T. We applied both the 'conventional' VA coupling approach, as well as this newer approach with the stiffness and temporal coupling indices.

Histopathological data collection

At the end of the protocol, the animal was killed with an intravenous injection of pentobarbitone (100 mg kg^{-1}). The heart was then rapidly harvested, rinsed with a cold isotonic saline solution and sectioned in five slices (0.6 cm thick) parallel to the atrioventricular groove from apex to base. Transverse tissue slices were rinsed with a cold isotonic saline solution and placed in 10% neutral-buffered formaldehyde. After 3 days of fixation, three or four tissue blocks were taken from each slice at standardized locations and routinely processed for paraffin histology. The tissue blocks from myocardium were cut at 6 μm, and each section was stained with Haematoxylin and Eosin (H&E) and Masson's trichrome. The stained sections were examined at magnifications of $\times$25, $\times$100, $\times$200 and $\times$400 to study the distribution of infarction. Photomicrographs were taken using a Zeiss photomicroscope (Axioscope 2 plus Sony 3CCD camera, 1024–768 pixels definition, Thornwood, NY, USA). In addition, tissue blocks of slice S3 were processed for immunohistochemical staining of desmin to investigate lesions of the cardiac muscle. Polyclonal antibodies to myoglobin (Dako, Glostrup, Denmark) were diluted 1:400. Monoclonal antibodies to desmin (clone D33, Biomeda, Foster City, CA, USA) were diluted 1:20. These methods to detect myocardial lesions were developed previously in other experimental protocols in the pig (Rolin *et al.* 2003; Dogné *et al.* 2005; Kolh *et al.* 2006).

Table 1. Overview of principal haemodynamic parameters

	Baseline (BL)	1 h ischaemia (T60)	1 h ischaemia + 2 h reperfusion (T180)	1 h ischaemia + 4 h reperfusion (T300)	Evolution with time
HR (beats min^{-1})	97.9 ± 15.6	106.4 ± 12.8*	120.6 ± 14.7*†	122.4 ± 20.0*†	$P < 0.001$
CO (ml s^{-1})	62.0 ± 11.3	59.8 ± 6.4	44.6 ± 7.0*†	44.0 ± 6.1*†	$P < 0.001$
EF (%)	54.5 ± 11.3	45.4 ± 9.0*	31.1 ± 5.0*†	32.4 ± 6.8*†	$P < 0.001$
MAP (mmHg)	96.7 ± 22.1	102.7 ± 22.5	88.1 ± 19.6†	78.4 ± 21.4*†‡	$P < 0.001$
EDV (ml)	75.0 ± 24.6	76.8 ± 13.3	73.1 ± 13.6	68.9 ± 11.1†	$P = 0.009$
ESV (ml)	35.8 ± 16.2	42.9 ± 13.2	50.9 ± 12.3*†	46.9 ± 10.4*†	$P < 0.001$
SV (ml)	39.2 ± 11.6	34.0 ± 3.8*	22.2 ± 2.5*†	22.0 ± 4.1*†	$P < 0.001$
SW (mmHg ml)	3600 ± 649	3200 ± 342*	1889 ± 442*†	1767 ± 567*†	$P < 0.001$
PVA (mmHg ml)	6657 ± 1382	5941 ± 1080	4586 ± 872*	3282 ± 876*	$P < 0.001$
SW/PVA	0.56 ± 0.06	0.55 ± 0.11	0.41 ± 0.09	0.46 ± 0.09	$P = 0.335$
E_a (mmHg ml^{-1})	2.75 ± 1.45	3.35 ± 1.60*	4.76 ± 2.11*†	4.57 ± 2.68*†	$P < 0.001$

Values are means ± S.E.M. Significant differences: *$P < 0.05$ *versus* baseline; †$P < 0.05$ *versus* T60 measurement; ‡$P < 0.05$ *versus* T180 measurements. Indicated *P* values show the statistically significant differences in the evolution with time of the different parameters.

Statistical analysis

Differences between the four measurements at baseline, after 1 h of ischaemia and after 2 and 4 h of reperfusion were tested with a general linear model for repeated measurements using SPSS software (SPSS Inc., Chicago, IL, USA). The model first revealed statistically significant differences in the evolution with time of the different parameters, with the level set at $P = 0.05$. If differences were present, *post hoc* tests were performed to detect at which instances in time the data were different. The Sidak confidential interval adjustment was used.

Results

Haemodynamic data (means ± S.E.M.) at baseline (BL), after 1 h of ischaemia (T60), after 2 h of reperfusion (T180) and after 4 h of reperfusion (T300) are shown in Table 1 and Figs 2–4.

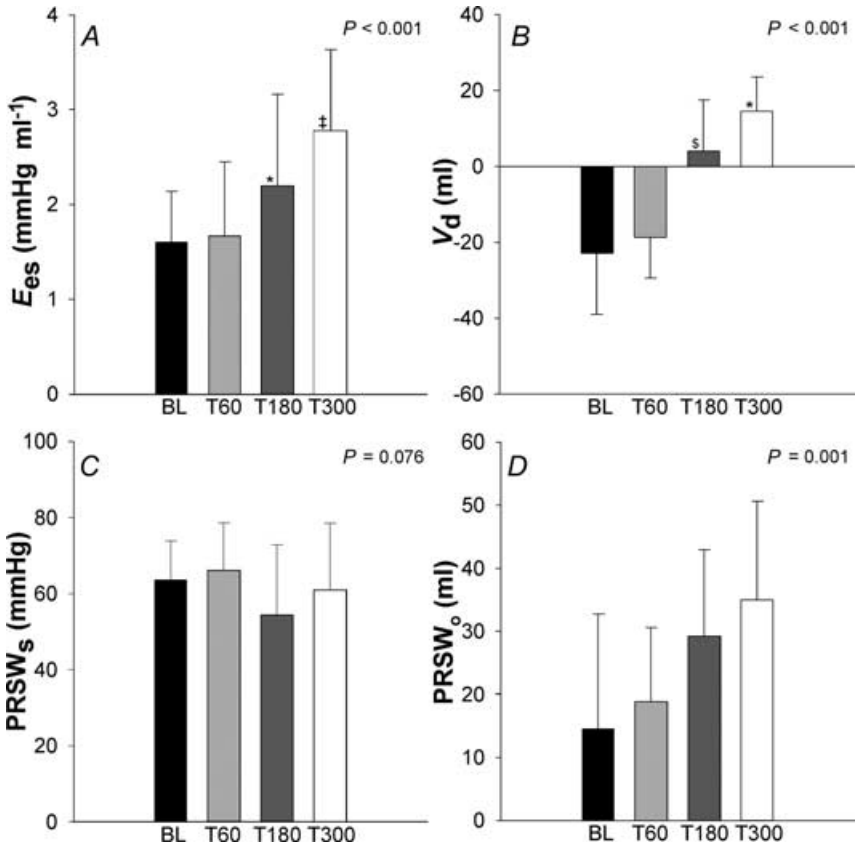

Figure 2. Left ventricular function parameters
The figure shows the end-systolic elastance (E_{es}, *A*), dead volume (V_d, *B*), the slope of the preload-recruitable stroke work curve (PRSW$_s$, *C*) and the intercept of the preload-recruitable stroke work curve (PRSW$_0$, *D*). All parameters are shown at baseline (BL), after 1 h of ischaemia (T60), after 2 h of reperfusion (T180) and after 4 h of reperfusion (T300). Significant differences: *$P < 0.05$ *versus* baseline; \$$P < 0.05$ *versus* T60 measurement. Near-significant differences: ‡$P < 0.06$ *versus* baseline. Indicated *P* values illustrate the statistically significant differences in the evolution with time of the different parameters.

Effects of acute regional ischaemia (comparing BL with T60)

Ligation of the LAD coronary artery induced an increase in HR from 97.9 ± 15.6 beats min^{-1} at BL to 106.4 ± 12.8 beats min^{-1} at T60 ($P < 0.001$). Cardiac output and mean aortic pressure (MAP) were not significantly affected by an hour of ischaemia, while EF decreased from 54.5 ± 11.3 (BL) to $45.4 \pm 9.0\%$ (T60; $P = 0.033$).

End-diastolic volume did not change significantly between BL and T60, but there was a trend towards elevated ESV (35.8 ± 16.2 ml at BL versus 42.9 ± 13.1 ml at T60, $P = 0.074$). Over the same time interval, SV decreased from 39.2 ± 11.6 ml to 34.0 ± 3.8 ml ($P = 0.001$).

Neither end-systolic elastance nor V_d changed significantly between baseline and T60. The slope ($PRSW_s$) and the intercept ($PRSW_0$) of the preload recruitable stroke work curve were not significantly affected by the ischaemia either (Fig. 2).

Stroke work decreased from 3600 ± 649 to 3200 ± 342 mmHg ml ($P = 0.002$), while pressure–volume area and mechanical efficiency (SW/PVA) did not significantly change between BL and T60.

As for vascular function, we observed that the only four-element windkessel parameter that demonstrated significant changes was characteristic impedance R_1, which decreased from 0.077 ± 0.018 to 0.060 ± 0.012 mmHg s ml^{-1} ($P = 0.001$) between BL and T60. Peripheral resistance R_2, C and L did not change significantly (Fig. 3). Effective arterial elastance (E_a) increased from 2.75 ± 1.45 to 3.35 ± 1.60 mmHg ml^{-1}, between baseline and T60 ($P = 0.007$).

Ischaemia did not affect the ratio E_{es}/E_a significantly, nor did it affect $E_{es}C$. The ratio R_2C/T, however, showed a significant increase from 2.081 ± 0.298 at BL to 2.500 ± 0.417 at T60 ($P = 0.009$), as seen in Fig. 4.

Effects of sustained coronary reperfusion (T180 and T300 *versus* T60)

Heart rate increased further after reperfusion (from 106.4 ± 12.8 beats min^{-1} at T60 to 120.6 ± 14.7 beats min^{-1} at T180; $P = 0.001$), while sustained reperfusion (T300) did not lead to a further increase. Compared with ischaemia (T60), reperfusion induced a decrease in CO (from 59.8 ± 6.4 ml s^{-1} at T60 to 44.6 ± 7.0 ml s^{-1} at T180; $P < 0.001$), and CO remained at this level up to T300. Ejection fraction decreased (from $45.4 \pm 9.0\%$ at T60 to $31.1 \pm 5.0\%$ at T180; $P < 0.001$) and remained at this low level during sustained reperfusion. Mean arterial pressure decreased from 102.7 ± 22.5 mmHg at T60 to 88.1 ± 19.6 mmHg at T180 ($P = 0.024$) and to 78.4 ± 21.4 mmHg at T300 ($P = 0.021$).

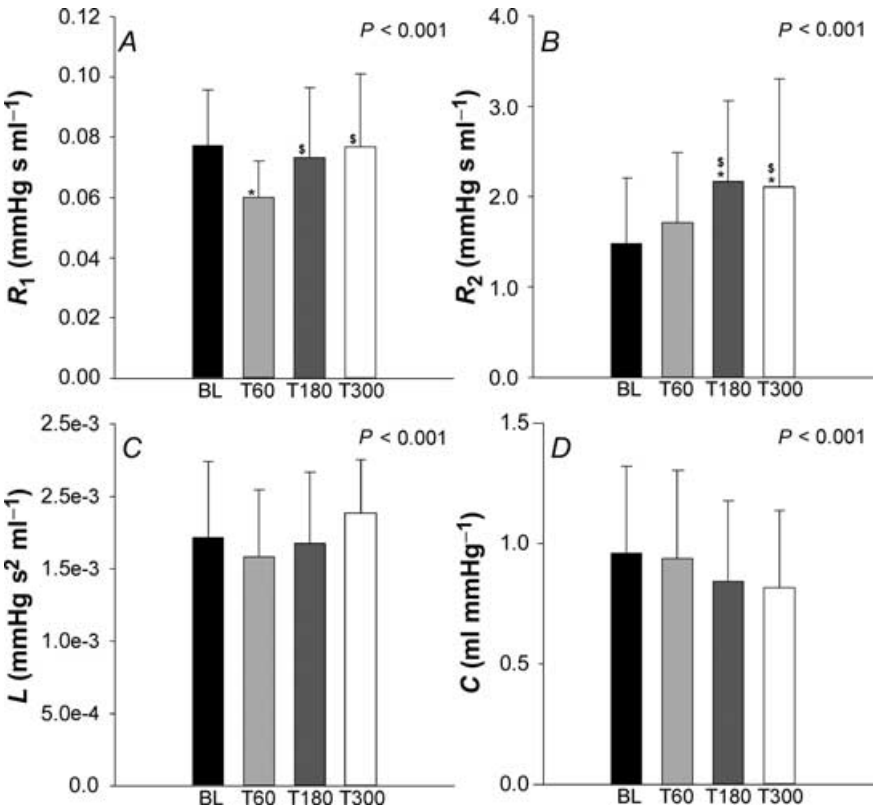

Figure 3. Arterial function parameters of the four-element windkessel model
The figure shows the characteristic impedance (R_1, *A*), peripheral resistance (R_2, *B*), blood inertia (*L*, panel *C*) and total compliance (*C*, panel *D*). All parameters are shown at BL, T60, T180 and T300. Significant differences: * $P < 0.05$ *versus* baseline; \$$P < 0.05$ *versus* T60 measurement. Indicated *P* values illustrate the statistically significant differences in the evolution with time of the different parameters.

While end-diastolic volume remained unchanged, ESV increased from 42.9 ± 13.2 ml at T60 to 50.9 ± 12.3 ml at T180 ($P = 0.014$) and did not further increase at T300. Coronary reperfusion induced a decrease in SV from 34.0 ± 3.8 ml at T60 to 22.2 ± 2.5 ml at T180 ($P < 0.001$). Stroke volume did not change further between T180 and T300.

End-systolic elastance (E_{es}) showed an increasing trend from 1.66 ± 0.79 mmHg ml^{-1} at T60 to 2.19 ± 0.97 mmHg ml^{-1} at T180 ($P = 0.063$) and did not show a further increase with sustained reperfusion. The dead volume (V_d) increased significantly from -18.70 ± 10.77 ml at T60 to 4.08 ± 13.46 ml at T180 ($P = 0.005$), but did not increase further with sustained reperfusion. The preload recruitable stroke work slope and intercept, in contrast, were not significantly influenced by coronary reperfusion.

Stroke work decreased as a result of early reperfusion, from 3200 ± 342 mmHg ml at T60 to 1889 ± 442 mmHg ml at T180 ($P < 0.001$), and did not change with sustained reperfusion. In the same interval, PVA and SW/PVA were not significantly affected by reperfusion.

Applying the four-element windkessel model, we observed that characteristic impedance R_1 increased significantly, from 0.060 ± 0.012 mmHg s ml^{-1} at T60 to 0.073 ± 0.023 mmHg s ml^{-1} at T180 ($P = 0.014$), after which R_1 remained constant (Fig. 3). Peripheral resistance R_2 showed a similar pattern, increasing from 1.71 ± 0.78 mmHg s ml^{-1} at T60 to 2.16 ± 0.89 mmHg s ml^{-1} at T180 ($P = 0.044$) and remaining at an elevated level with sustained reperfusion, while global vascular compliance C and inertance L remained unchanged. Effective arterial elastance (E_a) increased further to 4.76 ± 2.11 mmHg ml^{-1} at T180 ($P = 0.020$), and remained constant at T300.

When looking at the left ventriculo-arterial coupling (Fig. 4), no statistical changes were observed for the ratio E_{es}/E_a from T60 to T300, whereas the ratio R_2C/T increased further from 2.500 ± 0.417 at T60 to 3.261 ± 0.678 at T180 ($P = 0.023$), after which this parameter remained constant. The product $E_{es}C$ remained unchanged during the whole period.

Histopathological examination of infarcted myocardium

Histopathological examination revealed that main ischaemic changes were observed in the anterior left ventricle, corresponding to the area supplied by the LAD coronary artery. Reperfused myocardium displayed altered muscle cells, showing a waviness aspect which expresses prominent myofibrillar contraction bands, anisokaryosis and accumulation of interstitially infiltrated inflammatory cells as neutrophils and lymphocytes (Fig. 5*A*). Immunohistochemical detection of desmin revealed, mainly in the anteroseptal region, blurred zones where it was difficult to clearly delineate a necrotic zone from healthy myocardium owing to a motley appearance (Fig. 5*B*). Clear zones of patchy necrosis were also observed. The area not supplied by the LAD artery (posterior region) showed myofibrils with normal morphology.

Discussion

The main objectives for the study were twofold. Firstly, we wanted to gain more insight into the haemodynamic impact of the ischaemia–reperfusion mechanism. While much has been published on reperfusion injuries at the cellular level (Garcia-Dorado, 2004; Piper *et al.* 1998; Piper *et al.* 2004), little is known about its influence on LV global function, arterial function and VA coupling. Secondly, we wanted to verify whether pigs with acute coronary ischaemia, which were reperfused after 1 h, provide a useful large animal model for further study of pharmacological treatments to minimize reperfusion injuries.

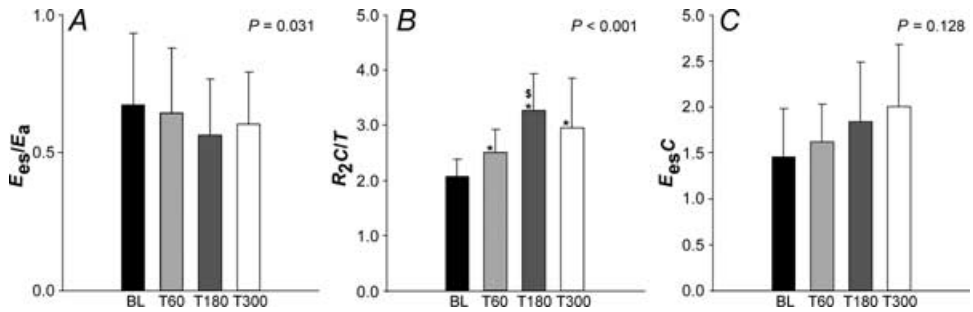

Figure 4. Ventriculo-arterial coupling
The figure shows the ratio E_{es}/E_a (*A*), the ratio of characteristic periods R_2C/T (*B*) and the ratio of total compliances $E_{es}C$ (*C*). All parameters are shown at BL, T60, T180 and T300. Significant differences: $*P < 0.05$ *versus* baseline; $\$P < 0.05$ *versus* T60 measurement; $\dagger P < 0.05$ *versus* T180 measurement. Indicated *P* values illustrate the statistically significant differences in the evolution with time of the different parameters.

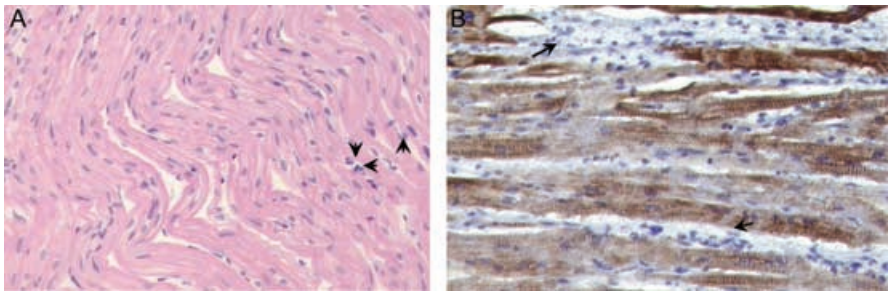

Figure 5. Histo pathological sections of infarcted myocardium
A, Haematoxylin and Eosin staining of a histological section from the anteroseptal region from a heart suffering from 1 h ischaemia followed by 4 h of reperfusion (original magnification, ×200). The wavy and stretched appearance of necrotic cells is seen. The nuclei of the muscle cells exhibit karyorrhexis and pycnosis. A few neutrophils are present (short arrows). *B*, immunohistochemical detection of desmin in the anterior region of heart suffering from 1 h ischaemia followed by 4 h of reperfusion (original magnification, ×200). Several myofibrils have a preserved pattern of cross-striation. An intense leukocytic infiltrate is present (arrows).

Pigs were used in this study because of the similarity between the hearts of pigs and humans concerning the anatomical distribution of coronary arteries, the lack of collateral circulation and the heart-to-body weight ratio (White & Bloor, 1981; Schaper *et al.* 1988). Open-chest preparation was used because it offers the advantage of a very strictly controlled induction of myocardial ischaemia and reperfusion using a clamp.

Ventricular systolic function and energetics

We assessed LV systolic function by the slope and intercept of the ESPVR and the PRSW, both of which have been demonstrated to be relatively insensitive to changes in preload and afterload (Suga *et al.* 1979; Glower *et al.* 1985). Our data illustrate some of the difficulties associated with the interpretation of these indices. An increase in contractility results in an ESPVR that shifts to the left and upwards (Suga *et al.* 1979), i.e. a decrease of V_d combined with an increase of end-systolic elastance, E_{es}. We anticipated that contractility would be depressed following myocardial ischaemia, but this was not reflected by the slope of the ESPVR, which increased throughout the protocol. The dead volume, however, shifted to the right, indicating a loss of contractile function (Fig. 2).

To better elucidate the net effect of concomitant changes in slope and intercept of the ESPVR, we calculated the maximal realizable pressure, P_{max}, the pressure that would be generated by the LV in a sustained isovolumic contraction at EDV: $P_{max} = E_{es}(\mathrm{EDV} - V_d)$. Figure 6*A* shows that an increase in E_{es} results in an increase in P_{max} (roughly equivalent to an increase in contractility), while an increase in V_d results in a decrease in P_{max} (roughly equivalent to a decrease in contractility). Clearly, increases in E_{es} as well as V_d, as seen in this study, have opposite effects on the maximal P_{max}. In Fig. 6*B*, we used averaged ESPVR values and calculated P_{max} using EDV data at BL, T60, T180 and T300. The increase in V_d and increase in

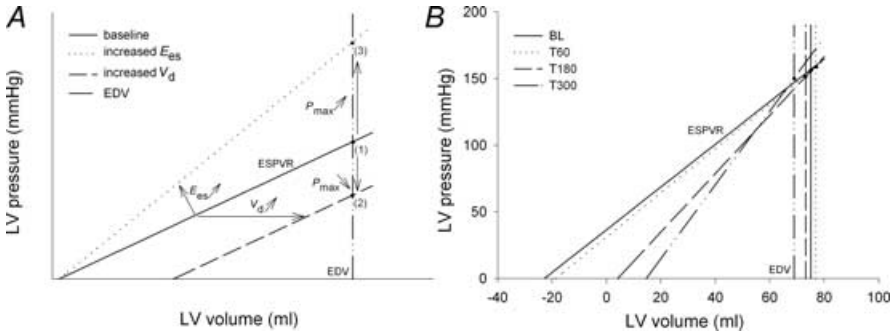

Figure 6. Ventricular systolic function parameters
A shows how an increase in dead volume (V_d) results in a drop of the maximum realizable pressure during isovolumic contraction, P_{max} (from point (1) to point (2)) and how the increase in end-systolic elastance (E_{es}) results in a rise of P_{max} (from point (1) to point (3)). *B* shows the end-systolic pressure–volume relationships (ESPVR) and the end-diastolic volumes (EDV), at BL, T60, T180 and T300. It is seen that the maximal realizable pressure during isovolumic relaxation does not change, because the increase resulting from an increase of E_{es} and the decrease resulting from an increase of V_d cancel out.

E_{es} counterbalance, and P_{max} remains unchanged. This finding is in line with the observation that the slope of the PRSW was virtually unchanged throughout the experiment. Note, however, that this does not imply that LV systolic function was unchanged. The higher E_{es} may be the result of elevated sympathetic tone in response to the ischaemia, using the functional reserve of the LV to withstand the effects of ischaemia and making LV function more sensitive to changes in volume and afterload. Also, there was a trend for an increase in the intercept of the PRSW. Since the end-diastolic volume did not change, this rightward shift of the PRSW with ischaemia and reperfusion will result in a drop of stroke volume, which was observed, and thus a drop of inotropy. These findings illustrate that when studying LV function, both the slope and the intercept of the ESPVR and PRSW should be taken into account to reveal a complete picture of LV function.

When taking a closer look at the ventricular energetics, a drop in stroke work is seen owing to ischaemia. Reperfusion causes SW to drop further, while stabilization is seen after sustained reperfusion. The drop in PVA, a measure for the oxygen consumption, is less pronounced and is only significant at T180 and T300. Since stroke work decreases more than pressure–volume area, a drop in efficiency would be expected, showing that more energy is dissipated, while less energy is transmitted to the blood. The changes are, however, too small to reach the preset level of statistical significance.

Histopathological data collection

So far, we have only discussed 'macroscopic' findings and effects on global cardiovascular function, and we found that reperfusion following ischaemia does not restore function. The sustained haemodynamic decline that is observed is in agreement with the histological findings, in which we also observed features of irreversible damage despite the reperfusion. The question is whether the damage results from the ischaemia or from the ischaemia and subsequent reperfusion (true reperfusion injury). In two (additional) animals that we killed after 1 h of ischaemia, we found signs of necrosis within the area at risk, suggesting that 1 h of ischaemia induced by LAD ligation is already sufficient to induce severe lesions in pigs. This is in accordance with the findings of Taylor *et al.* (1984), who also demonstrated that 1 h of ischaemia was sufficient to produce severe myocardial lesions in pigs. Like Taylor and co-workers, we believe that this probably results from the absence of a collateral circulation in the pig heart. We should nevertheless note that beyond the signs of necrosis observed, clear delineation between the reversible and the irreversible areas was not obvious even with immunohistochemical analyses, owing to the motley appearance of the staining in the myocardium from the anteroseptal region.

Arterial function

Besides LV function, we also addressed arterial function changes. Myocardial ischaemia (T60) does not affect systemic vascular resistance (R_2) which, together with a preserved cardiac output, results in an unaffected mean arterial blood pressure. However, an initial decrease of characteristic impedance R_1 is seen. Since R_1 depends merely on the elastic properties of the proximal aorta, this decrease, together with an unaffected mean aortic pressure, is suggestive of a (small) dilatation of the proximal aorta and/or decrease in aortic stiffness. With reperfusion (T180 and T300), R_2 increases, but because of the decrease in cardiac output, mean blood pressure decreases, resulting in higher R_1 (compared with T60) as the aorta will be less distended. Given the fact that sympathetic tone is likely to be elevated in these conditions, the higher R_1 may not be solely the effect of passive changes in aortic cross-section and function, but may also be modulated by changes in aortic vascular smooth muscle tone.

Ventriculo-arterial coupling

The coupling between the ventricle and the arterial system is commonly studied in terms of E_{es}/E_a. It has been argued, however, that E_{es}/E_a is not a very sensitive parameter (Segers *et al.* 2002). Another problem involves the use of E_a as representing arterial function, since E_a cannot be considered as a 'pure' arterial function parameter (Segers *et al.* 2002). In this study, ischaemia and reperfusion induced an alteration in ventricular and arterial function, yet the change in ventriculo-arterial coupling expressed using E_{es}/E_a was insignificant. This preservation of E_{es}/E_a may result from the fact that coupling is preserved, but it may also be a demonstration of the relative insensitivity of the parameter.

In this respect, it may be relevant to address coupling using the approach first advocated by Stergiopulos *et al.* (1996), who considered two independent coupling parameters, R_2C/T and $E_{es}C$, in order to assess the ventriculo-arterial coupling in a more elaborate model of the interaction between the LV and the arterial tree. The temporal coupling index R_2C/T relates the characteristic time periods of both the ventricle (T) and the arterial tree (R_2C). The product R_2C is the time constant of the arterial windkessel, and determines the time constant with which the pressure decays during diastole. In all mammals, R_2C/T is similar, which implies that the systolic-to-diastolic pressure difference (the pulse pressure) is constant. An increase in heart rate (smaller T) and R_2C/T allows less time for the arterial pressure to decay in diastole, with

higher diastolic pressures (coronary perfusion pressure) as a consequence. In a setting of myocardial ischaemia, elevated coronary perfusion pressures may be beneficial. The stiffness coupling index, $E_{es}C$, is in fact the ratio of the ventricular stiffness E_{es} and the arterial stiffness, $1/C$. This ratio may be more meaningful than the usually used E_{es}/E_a because E_a is not a pure arterial parameter (Segers *et al.* 2002) and better describes the compliance mismatch between the arterial tree and the ventricle. In this study, the ratio is not significantly affected by ischaemia or by reperfusion, so there are no significant relative compliance changes of the arterial tree compared with the maximal compliance of the left ventricle. At this point, it is hard to tell which of the two coupling frameworks is more appropriate. It is certain that, although E_a has the dimensions of stiffness, it is not a measure of arterial stiffness (Segers *et al.* 2002). It should also be pointed out that the E_{es}/E_a framework evolved from the analysis of cardiovascular function in the pressure–volume plane, where the dimension 'time' is not taken into account. Changes in heart rate are therefore not explicitly accounted for by E_{es}/E_a (although they are implicitly included in E_a). As such, the framework as proposed by Stergiopulos *et al.* (1996) may be better suited to detect the effects of subtle changes in arterial stiffness and timing, and to place these changes in a context of ventriculo-arterial coupling.

Limitations

It is obvious that this study has some stringent limitations. Firstly, since this study mainly focused on the haemodynamic alternations observed during ischaemia and reperfusion, only limited histopathological data were collected. Nevertheless, it is important to underline that oxidants and free radicals generated in the ischaemic and reperfused heart are key mediators in the pathogenesis of the injury (Zweier & Talukder, 2006). However, since accumulation of interstitially infiltrated inflammatory cells was observed at the histological level, no more complementary analyses were realized at the molecular level because biochemical dosages, histological analyses and electron microscopy data presented irreversible injury.

Secondly, our data indicate that in a pig model, 1 h of ischaemia may be too long when studying reperfusion injury. Confronting the histological findings with the haemodynamic data, it is hard to attribute the decline in cardiac function solely to reperfusion injury. It is likely that we observed a dynamic process with a complex interaction between myocardial stunning, myocardial hibernation and progressive necrosis of myocardial areas where irreversible damage has occurred. Acute experiments in an open-chest setting are probably too short to capture the time scale within which stabilization of events (and cardiac function) occurs. However, close monitoring of cardiovascular function, as we did in this experiment, is extremely demanding in a more 'chronic' experimental setting, and it is also not easy to differentiate the effect of the animal preparation and surgical interventions from the impact of ischaemia and subsequent reperfusion. Also, further exploration of ischaemia–reperfusion injury would require the necessary control experiments to differentiate effects of ischaemia from effects of ischaemia–reperfusion. In this context, we refer to previous work of Kolh *et al.* (2003, 2005) where, in a setting of sustained occlusion, it was shown that haemodynamic alterations took place primarily during the first half-hour of ischaemia, followed by a plateau phase that was maintained for 3 h. These findings thus support the assumption that the changes observed in the present study are not solely due to ischaemia, and that reperfusion injuries may play a role in the haemodynamic decline.

Conclusion

In conclusion, we have demonstrated that 1 h of ischaemia in a pig model induces haemodynamic alterations which are not reversed by reperfusion, but rather sustained and worsened. It is unlikely that these alterations are attributable to ischaemic injury alone, indicating that acutely ischaemic pigs provide a valuable large animal model for further study of pharmacological treatments to minimize reperfusion injuries. We have further demonstrated that studying ventriculo-arterial coupling through both a stiffness and temporal coupling index may provide more detailed insights than the more commonly used E_{es}/E_a ratio.

References

Baan J, van der Velde ET, de Bruin HG, Smeenk GJ, Koops J, van Dijk AD *et al.* (1984). Continuous measurement of left ventricular volume in animals and humans by conductance catheter. *Circulation* **70**, 812–823.

Boersma E, Maas ACP, Deckers JW & Simoons ML (1996). Early thrombolytic treatment in acute myocardial infarction: reappraisal of the golden hour. *Lancet* **348**, 771–775.

Cerra FB, Lajos TZ, Montes M & Siegel JH (1975). Hemorrhagic infarction: a reperfusion injury following prolonged myocardial ischemic anoxia. *Surgery* **78**, 95–104.

Denslow S (1996). Relationship between PVA and myocardial oxygen consumption can be derived from thermodynamics. *Am J Physiol Heart Circ Physiol* **270**, H730–H740.

Dogné JM, Rolin S, Petein M, Tchana-Sato V, Ghuysen A, Lambermont B *et al.* (2005). Characterization of an original model of myocardial infarction provoked by coronary artery thrombosis induced by ferric chloride in pig. *Thromb Res* **116**, 431–442.

Garcia-Dorado D (2004). Myocardial reperfusion injury: a new view. *Cardiovasc Res* **61**, 363–364.

Glower D, Spratt J, Snow TR, Kabas JS, Davis JW, Olsen C *et al.* (1985). Linearity of the Frank-Starling relationship in the intact heart: the concept of preload recruitable stroke work. *Circulation* **71**, 994–1009.

Grant B & Paradowski L (1987). Characterization of pulmonary arterial input impedance with lumped parameter models. *Am J Physiol Heart Circ Physiol* **252**, H585–H593.

Hearse DJ, Humphrey SM, Nayler WG, Slade A & Border D (1975). Ultrastructural damage associated with reoxygenation of the anoxic myocardium. *J Mol Cell Cardiol* **7**, 315–324.

Higo K, Sano J, Karasawa A & Kubo K (1993). The novel thromboxane A2 receptor antagonist KW-3635 reduces infarct size in a canine model of coronary occlusion and reperfusion. *Arch Int Pharmacodyn Ther* **323**, 32–49.

Kamimura R, Miura N & Suzuki S (2003). The hemodynamic effects of acute myocardial ischemia and reperfusion in Clawn miniature pigs. *Exp Anim* **52**, 335–338.

Khalil P, Neuhof C, Huss R, Pollhammer M, Khalil M, Neuhof H *et al.* (2005). Calpain inhibition reduces infarct size and improves global hemodynamics and left ventricular contractility in a porcine myocardial ischemia/reperfusion model. *Eur J Pharm* **528**, 124–131.

Kolh P, Lambermont B, Ghuysen A, D'Orio V, Gerard P, Morimont P *et al.* (2003). Alteration of left ventriculo-arterial coupling and mechanical efficiency during acute myocardial ischemia. *Int Angiol* **22**, 148–158.

Kolh P, Lambermont B, Ghuysen A, Tchana-Sato V, Dogne JM, Hanson J *et al.* (2005). Effects of dobutamine on left ventriculoarterial coupling and mechanical efficiency in acutely ischemic pigs. *J Cardiovasc Pharmacol* **45**, 144–152.

Kolh P, Rolin S, Tchana-Sato V, Petein M, Ghuysen A, Lambermont B *et al.* (2006). Evaluation of BM-573, a novel TXA2 synthase inhibitor and receptor antagonist, in a porcine model of myocardial ischemia-reperfusion. *Prostaglandins Other Lipid Mediat* **79**, 53–73.

Lambermont B, D'Orio V, Gerard P, Kolh P, Detry O & Marcelle R (1998). Time domain method to identify simultaneously parameters of the windkessel model applied to the pulmonary circulation. *Arch Physiol Biochem* **106**, 245–252.

Metzsch C, Liao Q, Steen S & Algotsson L (2006). Myocardial glycerol release, arrhythmias and hemodynamic instability during regional ischemia-reperfusion in an open chest pig model. *Acta Anaesthesiol Scand* **50**, 99–107.

Newby K (1997). Clinical outcomes according to time to treatment. *Clin Cardiol* **20**, III11–III15.

Opie LH (1989). Reperfusion injury and its pharmacologic modification. *Circulation* **80**, 1049–1062.

Piper HM, Abdallah Y & Schäfer C (2004). The first minutes of reperfusion: a window of opportunity for cardioprotection. *Cardiovasc Res* **61**, 365–371.

Piper HM, Garcia-Dorado D & Ovize M (1998). A fresh look at reperfusion injury. *Cardiovasc Res* **38**, 291–300.

Rolin S, Petein M, Tchana-Sato V, Dogne JM, Benoit P, Lambermont B *et al.* (2003). BM-573, a dual thromboxane synthase inhibitor and thromboxane receptor antagonist, prevents pig myocardial infarction induced by coronary thrombosis. *J Pharmacol Exp Ther* **306**, 59–65.

Sagawa K, Maughan L, Suga H & Sunagawa K (1988). *Cardiac Contraction and the Pressure–Volume Relationship*. Oxford University Press, New York.

Schaper W, Görge G, Winkler B & Schaper J (1988). The collateral circulation of the heart. *Prog Cardiovasc Dis* **31**, 57–77.

Segers P, Stergiopulos N & Westerhof N (2002). Relation of effective arterial elastance to arterial system properties. *Am J Physiol Heart Circ Physiol* **282**, 1041–1046.

Steendijk P, Van der Velde ET & Baan J (1993). Left ventricular stroke volume by single and dual excitation of conductance catheter in dogs. *Am J Physiol Heart Circ Physiol* **264**, H2198–H2207.

Stergiopulos N, Meister JJ & Westerhof N (1996). Determinants of stroke volume and systolic and diastolic pressure. *Am J Physiol Heart Circ Physiol* **270**, H2050–H2059.

Suga H, Kitabatake A & Sagawa K (1979). End-systolic pressure determines stroke volume from fixed end-diastolic volume in the isolated canine left ventricle under a constant contractile state. *Circ Res* **44**, 238–249.

Taylor IM, Shaikh NA & Downar E (1984). Ultrastructural changes of ischemic injury due to coronary artery occlusion in the porcine heart. *J Mol Cell Cardiol* **16**, 79–94.

Wang QD, Penrow J, Sjoquist PO & Ryden L (2002). Pharmacological possibilities for protection against myocardial reperfusion injury. *Cardiovasc Res* **55**, 25–37.

White F & Bloor C (1981). Coronary collateral circulation in the pig: correlation of collateral flow with coronary bed size. *Basic Res Cardiol* **76**, 189–196.

Zweier J & Talukder M (2006). The role of oxidants and free radicals in reperfusion injury. *Cardiovasc Res* **70**, 181–190.

Acknowledgements

This research was supported by grants from the ARC 94/99-177 of the Communauté Française de Belgique, from the Belgian National Fund for Scientific Research, and from the Leon Fredericq Foundation of the University of Liège. Philippe Kolh and Vincent Tchana-Sato were funded, respectively, by a postdoctoral grant and by a doctoral grant of the National Fund for Scientific Research, Belgium. Lieve Lanoye is funded by a BOF grant 011D09403 from Ghent University.